# Correction of Work Functions for the Absolute Auger Electron Spectroscopy: Experimental Evidence and PC Simulation

Y.Z. Jiang, R. Kato, K. Goto and R. Shimizu*
*Nagoya Institute of Technology, Gokiso-cho, Showa-ku, Nagoya 466-8555, Japan*
**Osaka Institute of Technology, Kitayama 1-79, Hirakata, Osaka 573-0196, Japan*
kgoto@system.nitech.ac.jp

(Received: September 18, 2003; Accepted: January 6, 2004)

For the true kinetic energy calibration of Auger electron spectroscopy (AES), the relative work function of the sample to the Auger electron analyzer (cylindrical mirror analyzer: CMA) must be corrected. First, the experimental evidence of phenomena of the work function for some typical materials has been shown, which is the characteristics in their secondary electron appearance thresholds. Then, the threshold of the secondary electrons with the sample bias was investigated, since the threshold of the secondary electrons has been believed to begin just above "0" of the vacuum level. The PC simulation concluded that the true energy distribution of the secondary electrons can only be obtained in a null field with straight trajectory to the CMA. But it showed the practical calibration of electron energies down to 10meV to be possible. Here all materials except the sample are coated with "soot" and an electrostatic shield, according to the PC simulation, is introduced just around the sample to make the correction by sample biasing. The PC simulation also revealed that sample having locally different work functions, such as polycrystalline, would tend to show their highest work functions. The careful observation of the energy distribution of the secondary electrons would discriminate the null field, thus this is a self-consistent correction method.

## 1. Introduction

A novel cylindrical mirror analyzer (CMA) [1], which is almost perfect for the reference AES that would be traceable to **SI** units both in energy and intensity, has been developed and examined. The true kinetic energy calibration referenced to vacuum level as zero energy with work function correction is, however, in progress as we consider that the true kinetic energy is of universal one. Energy calibration has been reported for XPS and AES [2], which employed the "Fermi edge" as a reference. Thus it should not be the true kinetic energy in the vacuum. Our database not having been completed but has been adopted in the project of Common Data Processing (Compro) of Japan.

The absolute energy calibration of tens of meV in AES by using elastically backscattered primary electrons can be feasible with an iterative method [3], which is automatically corrected for the peak energy position of the apparent thermionic emission of the electron gun, assuming the energy distribution to be constant for the energy range. This calibration is referenced to the vacuum zero level of the analyzer (CMA) provided the work function of the whole CMA is to be uniform. If the work functions of the CMA, coated with soot/carbon, and that of the sample are different, then an ambiguous value will be resulted. It is a quite common problem in AES and in other energy analyses as well. For the complete absolute energy calibration, the relative (absolute being preferable) work function of the sample to the CMA must be corrected or compensated.

Measuring techniques of the work function fall into two general categories: (1) relative and (2) absolute measurement methods. In the former (1), the work function of the reference surface must be known or measured in advance. The Kelvin-Zisman method is very popular. It is a non-contact capacitor device having been introduced by Lord Kelvin in 1898 [4] and modified by Zisman with vibrating probe with a feedback circuit in 1932 [5]. The general limitations of this method are the need a reference electrode and the effect of stray capacitance.

Absolute measurement methods include those of the photoelectric emission [6], the thermionic emission [7], and the field emission [8]. Photoelectric emission method [9] is the only practical method to obtain an absolute work function. But it can not be easily obtained by detecting a faint onset threshold of the photoelectron yield. Thus the background should be as small as possible, such a level of $10^{-4}$ or $10^{-6}$ being advisable [6]. High background would tend to give a higher work function values. Further the

Copyright (c) 2004 by The Surface Analysis Society of Japan

sample having locally different value for work functions, such as the polycrystalline one, would also tend to show the highest work functions. In the separate experiments (Li *et.al.*), we are successfully performing a study of absolute work function by photoemission with a modified photoemission electron microscope (PEEM). A steady value has been obtained.

Secondary electron (SE) emission results when high-energy electrons, photons or ions are colliding with a surface. Several authors have proposed methods to evaluate work function with Auger electron spectroscopy by using onset energy of SE emission [10], [11] and [12]. Since the SE threshold energy is the lowest value of kinetic energy that electrons from the sample can have and be analyzed and it has been believed to begin just above "0" of the vacuum level. In other words, there will be a shift in the thresholds of SE according to the relative work function of the sample to the CMA. That means if the relative work function of the sample to the CMA can be completely compensated, then the true SE spectra can be obtained. But the energy distribution of SE and consequently the threshold can not be measured easily. To improve the sensitivity, an acceleration bias voltage is often used. But this would normally make the energy distribution of SE change, thus special care was paid in the measurements [10].

We will introduce a self-consistent correction method to compensate the difference in work functions by using a sample bias voltage; one kind of SE method.

## 2. Experimental

A novel prototype CMA [1] of almost calculable ($\Delta E/E = 0.25\%$) has been used for our experiments. The basic designs have been given [13] and quite a similar CMA with us also been calculated [14]. The experimental arrangement is shown schematically in Fig.1, of which the electron gun, the sample holder, the slit and electric shields have been improved recently [3, 15].

By the improved electron gun with an extractor, the energy distribution of primary electrons, *i.e.*, the shape and the peak position, would be kept constant irrespective of the acceleration voltage of primary electrons. With this setup and an introduction of an iterative method, we can calibrate the CMA on a kinetic energy scale. Similar results can be obtained by simple calculation, *i.e.*, the offset function method, since the peak position seems as an offset function in the calibration [16]. The iterative method is a key factor for our study. A part of the sample holder is made of a quartz tube to reduce the thermal expansion due to the sample heating by the primary electron beam, since 1 $\mu$m of the relative expansion is affective. An extra baffle slit (S2) was set and the reduced ghost spectrum of less than $10^{-4}$ was obtained [17]. The Wehnelt is made of $\mu$ -metal and the wiring of the cathode is twisted to decrease and cancel the generated magnetic field. With dual $\mu$ -metals, electron energy distribution of whole range of the primary electrons through true SE of 1eV or below can qualitatively be detected by electrometer (Keithley model 642; SI traceable).

The CMA is coated with soot to reduce the electron scattering and we would obtain a stable and uniform work function of the CMA. The stability of the coating is now under study by irradiating the surface with argon ions and electrons. A $\mu$ -metal patch (PC-78, thinness 0.3mm) with a hole (18mm diam.) in the center is attached to the entrance of the internal $\mu$ -metal shield for the minimal magnetic field (0.1mG or below) for the sample and CMA. This will lead the definition of the slow true SE to be clear. The sample used in this study is incidentally polycrystalline Mn, which is slightly oxidized but stable. To apply the sample bias voltage and to measure the sample current accurately, a

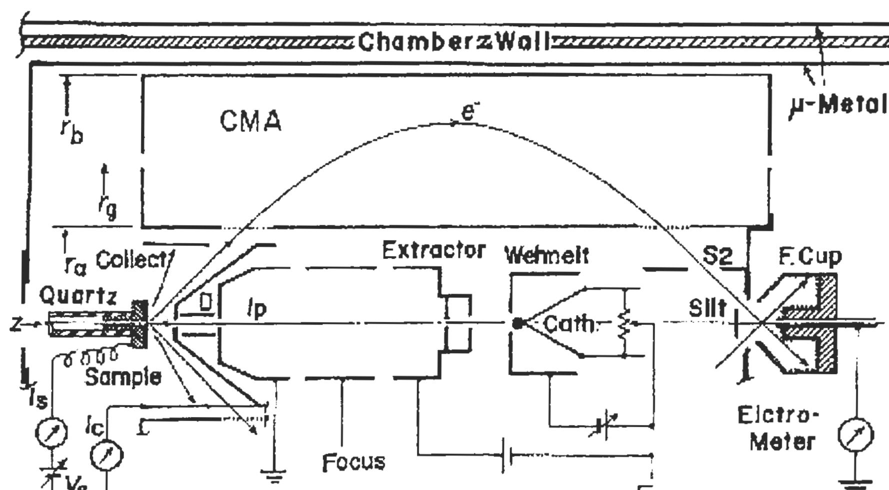


Fig.1. Schematic experimental arrangement

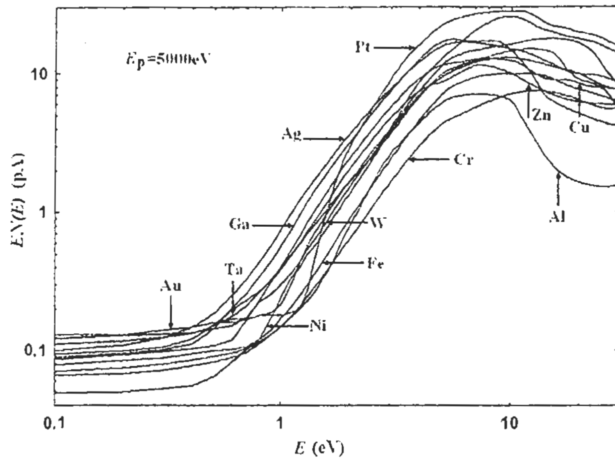


Fig.2. The onset of SE energy distribution in "log-log" plot for several typical elements for $Ep$=5000eV.

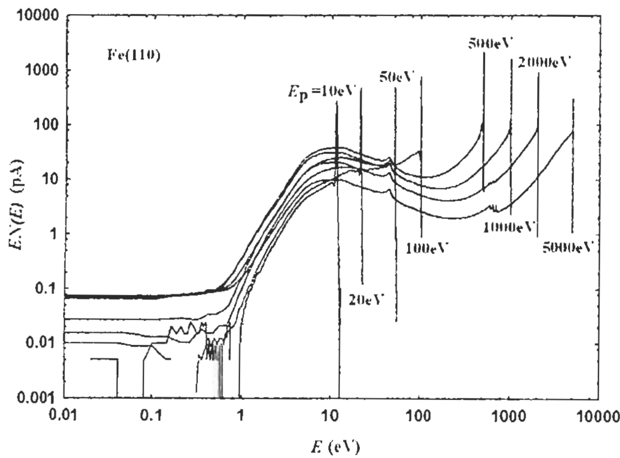


Fig.3 Total spectra of Fe (110) for $Ep$ = 10eV ~ 5keV.

triaxial and guard method was employed.

The relationship between the onset of secondary electrons and the sample bias voltage was investigated [18]. Then the electric fields around the sample and the SE trajectories were simulated by PC and an introduction of an electrostatic shield was proposed for the better definition of the slow true SE.

## 3. Results and discussion

In order to make effects of work function clear, a log-log plot which we call "advanced Sickafus plot" which can show all materials and energies in one sheet [19] is used. The onsets of true SE energy distribution for several typical materials, are shown in Fig. 2. The intensity, $EN(E)$, is normalized to the 1 μA of primary electron current. It should be noted that the spectra ranging 0.1~10eV would show the characteristics relating to the work function difference, interband transitions, and structures due to the plasmon excitation in the true SE range. The almost flat characteristics in the range 0.1-1eV were consisted of the rubbish electrons, *i.e.*, background, in the CMA. The flat curves and the true SEs did cross at each individual curve of the material. This can be an evidence due to the work function differences. Particularly, the sudden deflection observed in Pt just above 1eV was caused by the acceleration of SE to the CMA by the work function difference, as the work function of the Pt is the highest in the shown materials.

Fig. 3 shows the whole range of energy distribution of Fe (110) by changing the accelerating voltages from 10eV to 5000eV. The unusually large noises in the energy range below 1eV were arisen from the enhancement of the intensity for the normalization, since the primary electron current was very small as the order of nano amperes. If we move the spectra in parallel along the ordinate, they did converge almost to the same shape around 1eV. Quite the identical feature was found for other materials.

From the above results, we know that the work function change can lead to the simultaneous change of the threshold of the SE. Thus a sample bias method can be introduced. Fig. 4 would reveal the relationship between the onset of SE and the sample bias voltage. By changing the sample bias ($V_s$) from -1.0 V to 1.0 V in every 0.1 V, for $E_p$=50 V, we

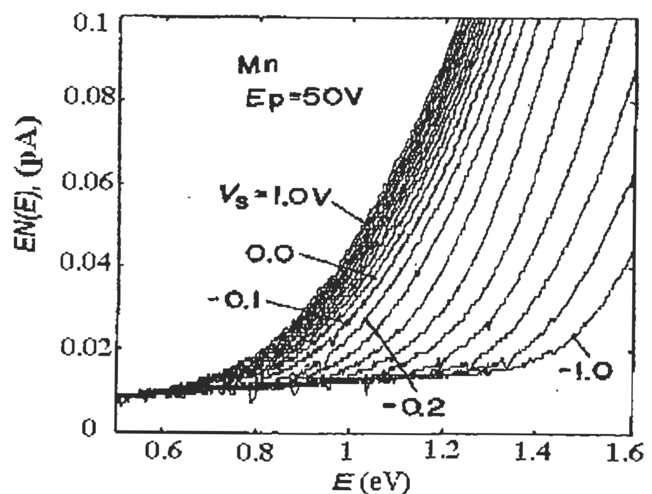


Fig.4 The true slow SE spectra as a function of the sample bias ($Vs$), for $Ep$=50eV.

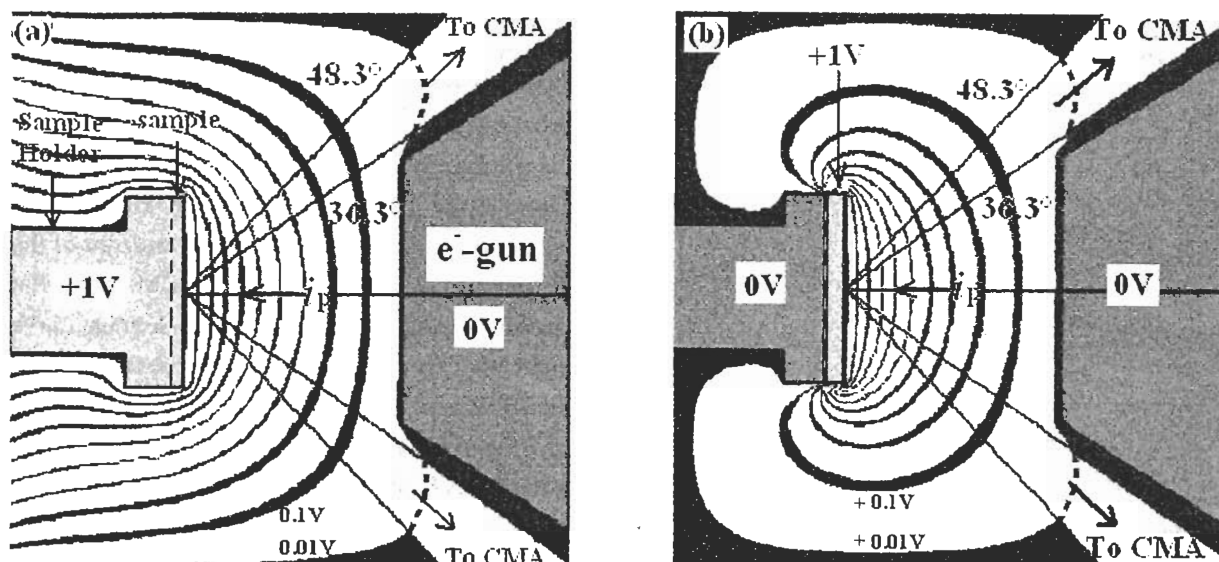


Fig.5 Simulation of the electric field distribution (10 divisions) around the sample; the sample and sample holder consist of the same work functions (a) and different one's (b).

obtained the energy distributions of SE of Mn. The characteristics began to concentrate at $V_s$ of about -0.1V~-0.2V, *i.e.*, the border between the modes of acceleration (coarse) and the deceleration (fine) for the SE by the retarding potentials between the sample and the CMA. We urged to find this critical voltage, because it should correspond to the true energy distribution of the SE, provided that the trajectory of the SE is straight.

## 4. Simulation

Figs. 5 (a) and (b) show the electric field distribution (10 divisions) around the sample simulated by PC for our present system. It was assumed that the all CMA system was consisted of the materials of the same surface potential, *i.e.*, the work function and the sample holder alone can externally be biased separately. The Fig. 5 (a) shows the distribution that the sample and sample holder have the same surface potential of other than the surroundings, *i.e.*, CMA system. Fig. 5 (b) shows the case that the sample holder has the same surface potential with the CMA system but the sample has different surface potential (work function). The two figures showed distinct difference, however the potential difference between the sample and the CMA system was the same. It was quite obvious from Fig. 5(b) that the lines of equipotential near the border of the sample and sample holder concentrated, as the surface potential abruptly changed. This abrupt change should affect the electric field of the electron trajectories. In a detailed comparison of the two cases for the electron trajectories to the CMA, we can find some differences in the electrical field maps. We must obtain a null field for both cases. Our conclusion is that the sample bias alone can not compensate the electric field in the system of different surface potential. Some elaboration of a shielding and sample biasing must be needed for the compensation.

We can get the null field by adjusting the sample bias only when the sample and the sample holder have the same work function. This is quite easy. But it was found that it might be a considerable work to obtain a null field in the other case that the sample has a different work function with the CMA system, Fig. 5(b). This is common in the laboratory. We considered to effectively shield the potential difference by introducing an electrostatic shield. This may eliminate the effect. Fig. 6(a) ~ (j) show the simulations of the equipotential distribution (100 divisions except one 1000 division, *i.e.*, +0.001V) around the sample with some variation of electrostatic shields. The sample was biased by voltage +1V for the relative work function of -1V of the sample. The surface potential of the shield and any other electrodes except the sample were assumed to be "0". These distributions can be applied for any other potential differences as their ratios. Our criterion was 0.01V of space

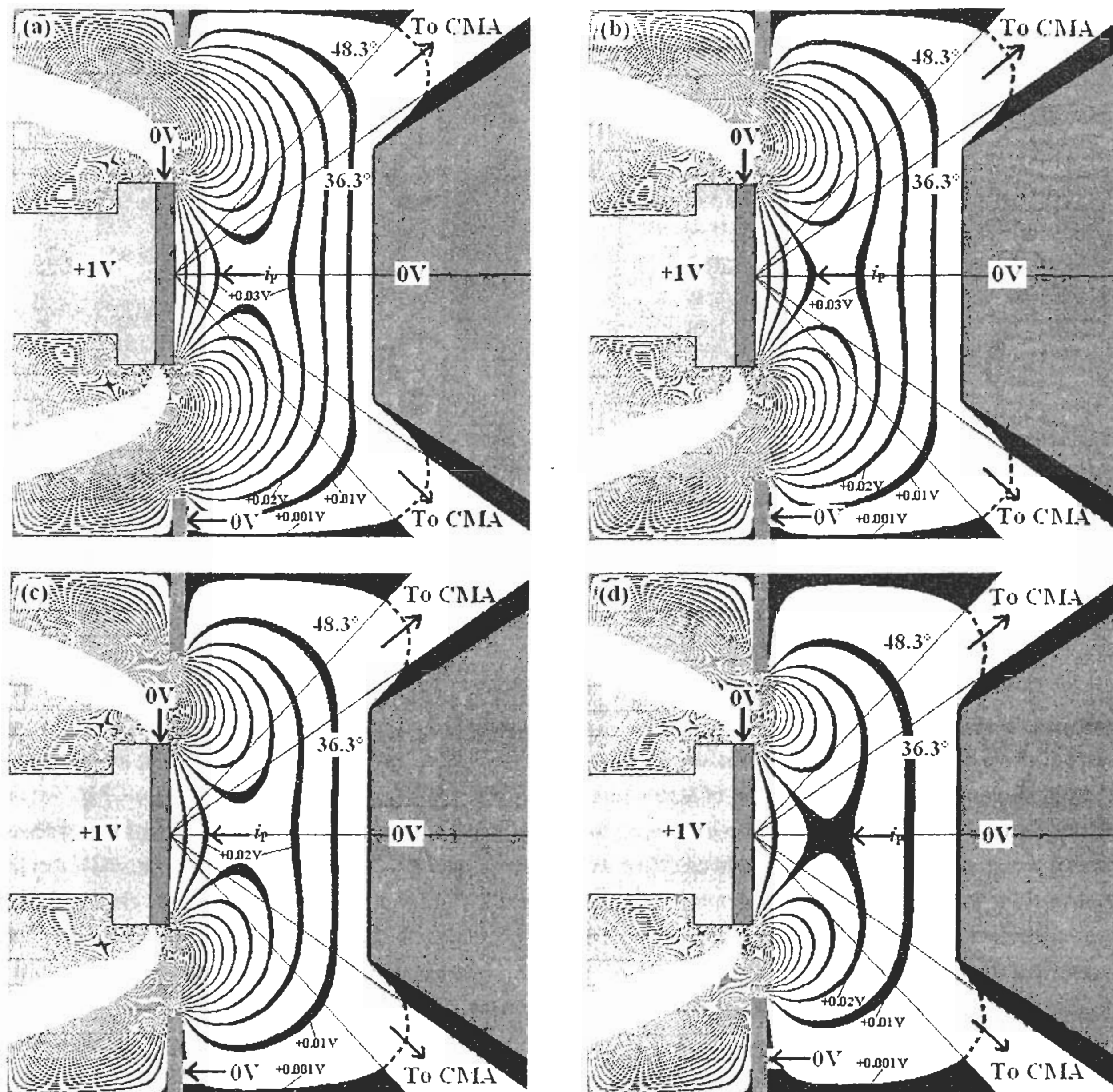


Fig. 6 The electrostatic equipotentials are around the sample for the annular shield diameter and position. The sample was biased by +1V as the work function difference between the sample and the vicinity was -1eV. The diameter and thickness of the sample were assumed to be 1 and 0.1, respectively. The diameter and position(from the sample surface) of the annular slits were correspondingly, (a)2.5, 0; (b)2.2, 0; (c)2.0, 0; (d)1.8, 0; (e)1.6, 0; (f)1.4, 0; (g)1.6, 0.1; (h)1.6, 0.2; (i)1.0, 0.2; (j)0.8, 0.2.

in the electron trajectories, so that Fig. 6(f) and Figs. 6(i) and (j) were acceptable. The design of Fig. 6(i) may be optimum for an actual experimental operation, because we should need some margin. In the more critical work, the Fig. 6(j) would be advisable. Any shapes and positions between Fig. 6(f) and Fig. (j) can be considered as equivalent optimum designs.

When the true SE undergoes the null field, which results in a straight trajectory to the CMA, then the true SE would be shown with the lowest threshold.

In order to prove the validity of the electrostatic shield, trajectories of SE were simulated. Only the upper halves of the trajectories are shown in Figs. 7 and 8 for the electron energies of 20meV and 10meV, respectively. The trajectories

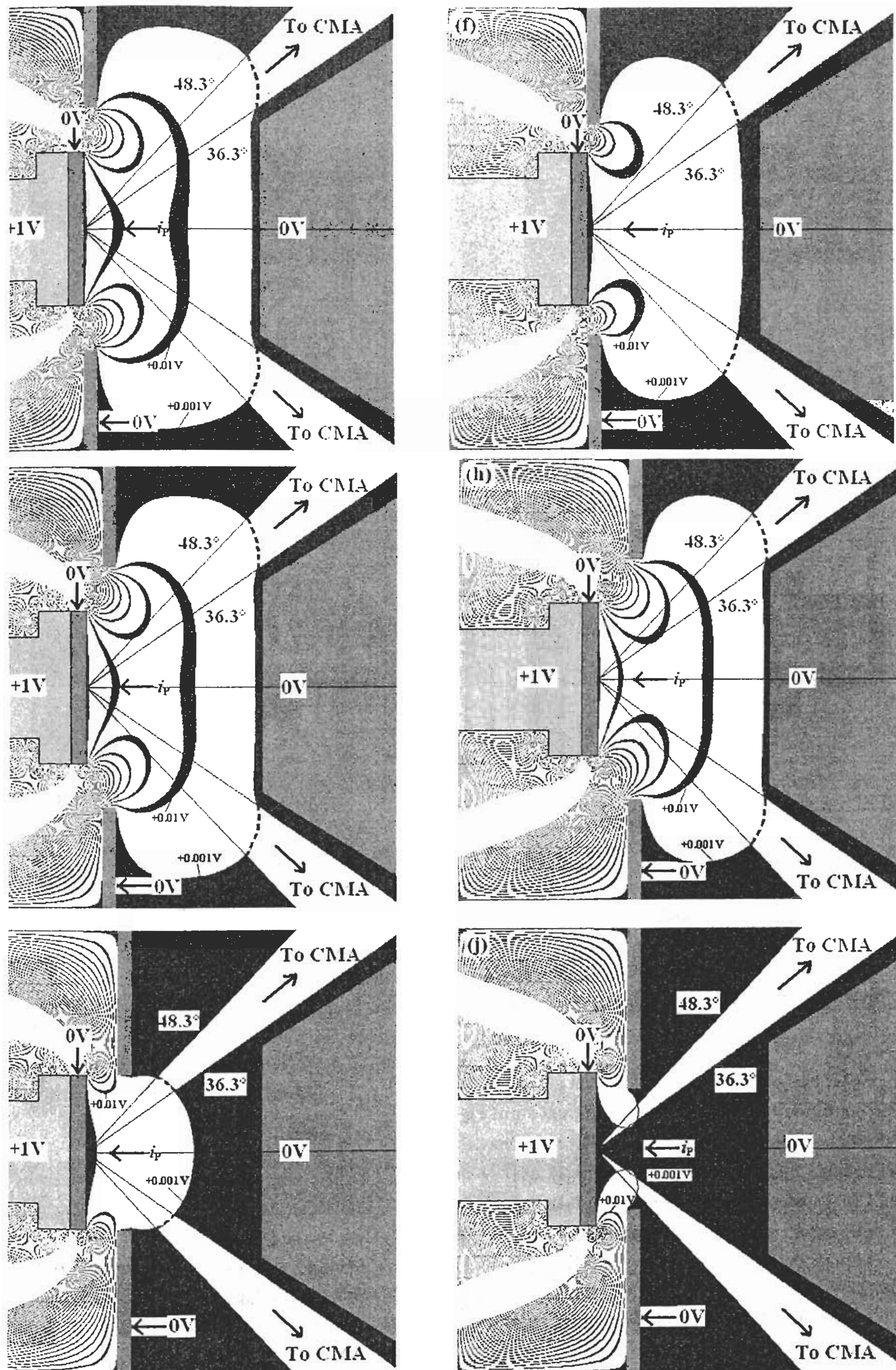
(f)
(h)
(j)
To CMA
To CMA
48.3°
36.3°
0V
+1V
$i_P$
+0.01V
+0.001V

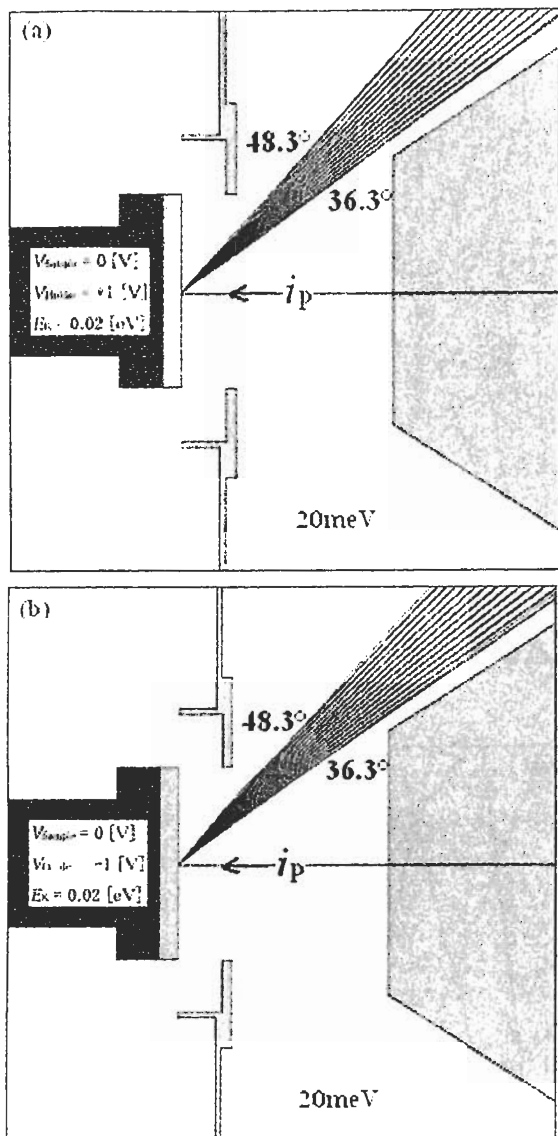


Fig.7 Trajectories of electrons (20meV) for sample biases with electrostatic shield. Sample is biased -1V(a) and +1V(b) to compensate the relative work function of +1eV and -1eV, respectively.

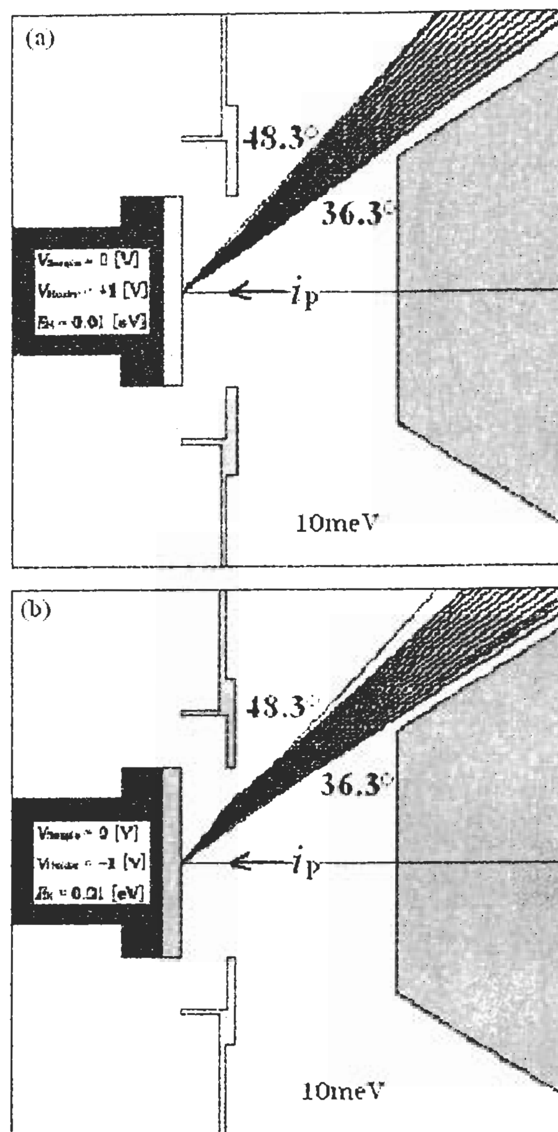


Fig.8 Trajectories of electrons (10meV) for sample bias with electrostatic shield: Figures correspond to those in Fig. 6(i).

for higher electrons were also studied, but not shown here. The configuration was somewhat different from Fig. 6 though no practical effect would exist. The upper ones (a)'s in these four figures have -1eV of lower work function than the CMA system then thus the sample bias was +1V for compensation; while the corresponding lower ones (b)'s

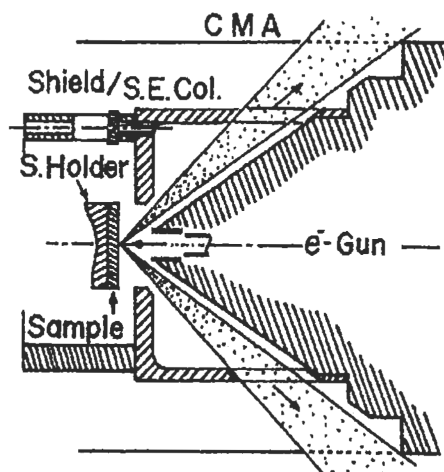


Fig.9 (Right) An actual electrostatic shield around the sample.

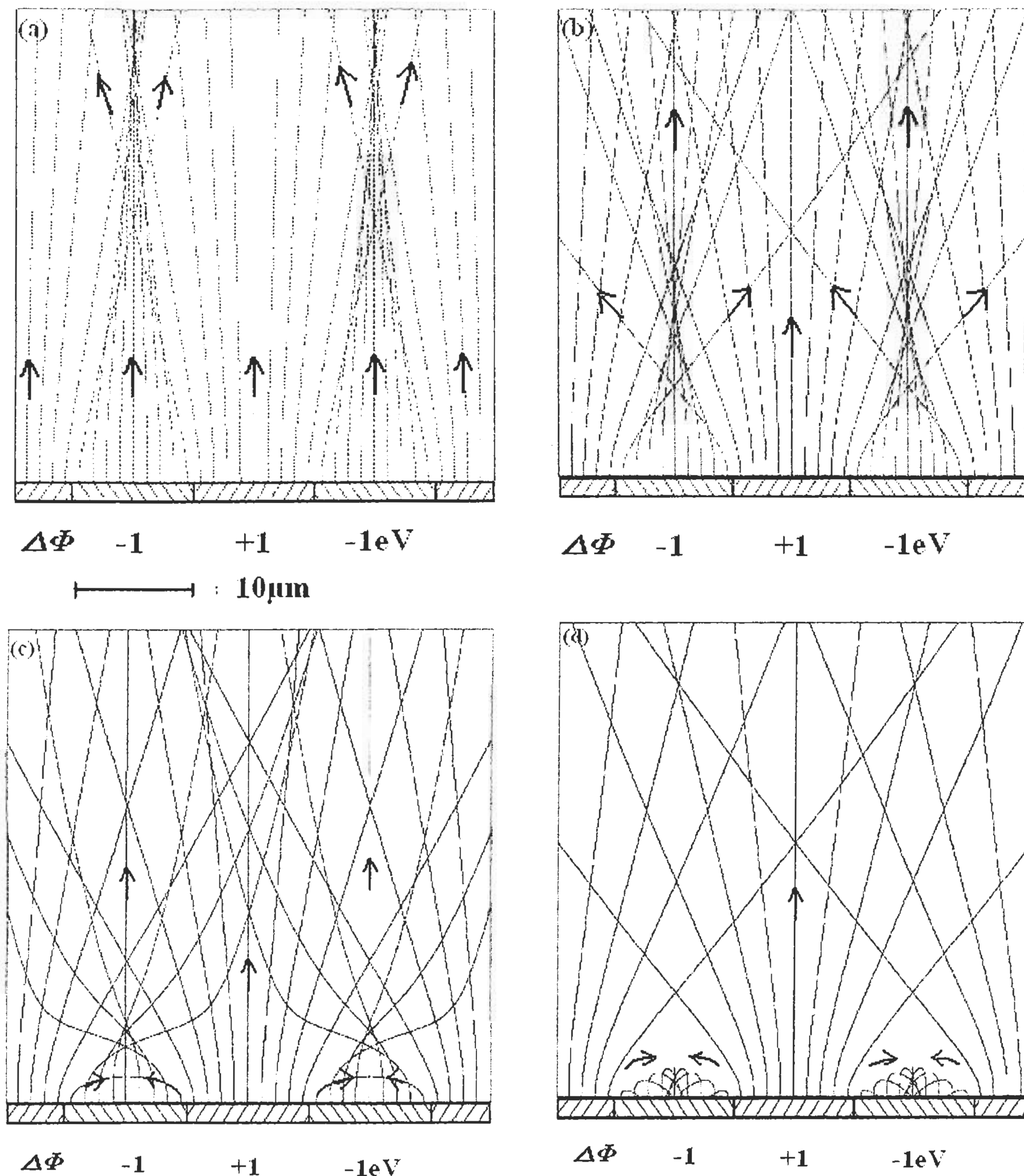


Fig.10 Trajectories of electrons emitted from the surfaces of relative work function of ± 1eV; (a) 5eV, (b) 2eV, (c) 1eV, and (d) 0.5eV in kinetic energies at the surfaces.

have +1eV of higher work function and the sample bias was -1V. From these results, we would see that for the electrons of 20meV or higher, no trace except of the ideal ones (emission angle of 42.3°±6°) can be found. While for those of 10meV, there we found no electrons of out of the ideal path with +1V of bias and only 20~30% are out of ideal path with -1V sample bias. These were the results duo to the complicated residual electric fields. So with careful

investigation of the spectra of SE, the correction of work function can be possible in the energy range of 10meV.

According to the simulations above, an electrostatic shield is introduced in our instrument. It is just around the sample and all materials (consist of Al and Cu) excepting the sample are coated with soot/aquadag. Fig. 9 shows a schematic shape and position of the electrostatic shield, secondary electron collector, and cone of the electron gun in our CMA. These are electrically connected together and all electron current to them can be measured by an electrometer. The scale of the sample is 10-mm in diameter and 1-mm thick.

All results that we have obtained above were for the case of the sample has a uniform work function over the surface.. It is not always suitable for the sample having locally different work functions, for example, polycrystalline of various faces over the surface. Simulation for the samples having different work function differences of ± 1eV are shown in Figs. 10(a) ~ (d), with kinetic energies (for the electrons at each surface, perpendicular to the surface of the sample) 5eV, 2eV, 1eV and 0.5eV, respectively. Suppose local work function of the sample changed varying from +1eV to -1eV with each interval of 10 μm and the environment of the sample was field free. This setup might be rather crude but will be a good measure of estimation. Figs. 10(a) and (b) show the electron tracks for the kinetic energies of 5eV and 2eV, respectively. Accelerated electrons from the sample surface of high value of work function would flight diverging. On the other hand, decelerated electrons from the sample surface of lower work functions would tend to converge. Particularly, the electrons that do not have enough kinetic energy (<1eV) to overcome the electric force would be driven back to the original grain, Fig. 10(d). Intermediate stage is shown in Fig. 10(c).

So when a sample has different work functions in it, it is clear that the observed threshold of SE is only composed of the electrons coming from the sample surfaces of highest value work functions. Because of the diverging tracks of electrons, only a fraction of those can be measured. This would make the threshold quite vague to be detected. For this reason, the highest work functions might have been reported.

## 5. Summary

With the iterative method [3], the energy calibration of tens meV in AES has already been feasible. This calibration is referenced to the vacuum zero level of the analyzer (CMA) and self-consistent. The correction for the relative work functions of the sample and the analyzer can be made by the sample bias method with a suitable electrostatic shield. With careful investigation of the onset characteristics of the secondary electrons with our improved instruments, the true secondary electron energy distribution can be obtained and consequently difference in the work functions can be compensated by the sample bias method. The energy correction of 10meV may be feasible. This is also a self-consistent correction for the absolute calibration like as in the iterative method. By combining the two methods complete absolute kinetic energy calibration will be in our hand.

## 6. Acknowledgement

We would like to sincere thanks to Dr. M.P. Seah of NPL, Dr. C.J. Powell of NIST. This work has been supported by the aid of the Special Coordinated Research of Science and Technology through NRIM (now NIMS) and the fund from NMC. One of the authors, Jiang would like to thank the Hori Information Science Promotion Foundation and the Monbushou of Japan government for the scholarships.

## References

[1] K. Goto, N. Sakakibara, Y. Sakai. *Microbeam Anal.* **2**, 123(1993).

[2] M.T. Anthony and M.P Seah. *Surf. Interface Anal.* **6**, 95 (1984); **6**, 107 (1984).

[3] K. Goto, N. Nissa Rahman, Y.Z. Jiang, Y. Asano and R. Shimizu. *Surf. Interface Anal.* **33**, 245(2002).

[4] Lord Kelvin, *Phil. Mag.* **46**, 82(1898).

[5] W. A. Zisman. *Rev. Sci. Instrum.*, **3**, 367(1932).

[6] C. Sebenne, D. Bolmont, G. Guichar, and M. Balkanski. *Phys.Rew.*, **B12**, 3280 (1975).

[7] H. Shelton. *Phys. Rev.*, **107**, 1553(1957).

[8] A. G. Knapp. *Surf. Sci.* **34**, 289(1973).

[9] For example in Rev., G. Margaritondo, Phys. Today. Apr. 66 (1988).

[10] B. Heuke, J.A. Smith, and D.T. Attwood. *J. Appl. Phys.* **48**, 1852 (1977).

[11] A. P. Janssen, P. Akhter, C. J. Harland and J. A. Venables. *Surf. Sci.* **93**, 453(1980).

[12] M. Yoshitake, K. Yoshihara. *Sinkuu.* **42**, 290(1999).

[13] V.V. Zashkvara, M.I. Korsunski, and O.S. Kosmachev, Sov. Phys.-Tech. Phys. **11**, 96 (1966).

[14] K. Goto. *J.Surface Anal.* **9**, 18(2002).
[15] K. Goto, Y. Z. Jiang, N. Nissa Rahman, Y. Asano and R. Shimizu. *Surf. Interface Anal.* **34**, 211(2002).
[16] D. Fujita and K. Yoshihara. *Surf. Interface Anal.* **21**, 226 (1994). And M. Suzuki, T. Maruyama, Y. Ohtsuka, M. Koizumi, M. Nagoshi, and T. Sekine. *J. Surface Anal.* **3**, 589 (1997).
[17] N.Nissa Rahman, K.Goto, and R.Shimizu, *J.Surface Anal.* **8**, 2 (2001).
[18] Y.Z.Jiang, W.L.Li, K.Goto, and R.Shimizu, *J. Surface Anal.* **9**, 348(2002).
[19] M.P. Seah. *Surf. Sci.* **17**, 132 (1969); and Y.Z.Jiang, K.Goto, and R.Shimizu, *J. Surface Anal.* **8**, 147 (2001).

**Excerpt from the discussions with the reviewers, added by the editor.** The figures etc. refered to below incdicate those in the original manuscript.

**Reviewer:** A brief evaluation is recommended to be included comparing the "true kinetic energy calibration method" described in the manuscript and the "Fermi edge" energy calibration method used widely in AES and XPS. Consider e.g. the case when the Auger electrons are excited from a (e.g. Si) substrate covered by an (e.g.) oxide overlayer or the case when the same Auger transition is excited from different orientation grains (different work functions) of a polycrystalline material, and detected as a function of the emission angle related to the surface normal.

**Authors:** The complicate surface will necessarily include larger uncertainty. Probably complicated materials shall be out of the category of standard and need a further study.

**Reviewer:** An estimate of the minimum value of magnetic field at the sample surface affecting appreciably the accuracy of the energy calibration method described, would be useful to include.

**Authors:** It is very hard work to measure the magnetic field in the CMA as low as below 1 mG. We measured it with a Mag Probe (F. W. Bell, 227mm length) which magnifies the normal Hall probe by 100 by the aid of the μ-metal, *i.e.*, sensitivity 0.01 mG. A care should, however, be paid to use it, as small residual magnetic field in the μ-metal may remain.

**Reviewer:** .Fig.3
Two spectra (acceleration energy of 500 and 1000eV) look to have lower threshold energy. Is it true? And if it is, why do they?

**Authors:** Yes. You are right. It might be an experimental matter of the time constant and sweep speeds. They should be the same.

**Reviewer:** .Results, page 3 line 2 from the bottom
Do the authors say that spectra of Cu(100), Cu(110) and Cu(111) near secondary threshold had similar characteristics? Does it mean that it is impossible to distinguish one crystal orientation from the three with this secondary threshold measurement?

**Authors:** Yes. We mean they have similar characteristics near secondary threshold. It is mainly because work functions in the different crystal orientation of a polycrystalline have small difference, and the secondary electrons may have structure dependant characteristics .

**Reviewer:** Fig.5-6
The coloring of the figures is confusing.
In Fig.5(a), the potential of the sample holder and the sample is same and that potential is different from the surroundings. It is clear from the figure as the sample holder and the sample has the same, red color and the color near 'e-gun' is blue. In Fig.5(b), the color of the sample holder and near 'e-gun' are red and that of the specimen is blue. Does it mean the potential of the sample holder is same as (a) and that of surroundings is adjusted to the sample holder and sample potential is changed to the potential of surroundings in (a)? I do not think so. Please take great care in coloring. I know that the equi-potential lines are same, but to make readers understood the figures, the coloring should be revised. It is difficult to find what is the difference between Fig.6(a) and Fig.6(b). All the color is vice versa. If Fig.6(a) corresponds to Fig.5(a), the color near 'e-gun' should be same, isn't it?

**Authors:** I. We changed the colors to the corresponding black and white.

**Reviewer:** .Simulation, page 4, line 2 from the bottom
Because the shielding is the most important point of this

paper, please give figures of shapes and sizes of calculated shields.

**Authors :** The simulations of Fig.6 and with some variations (not shown), Fig.7 and Fig.9 showed quite identical shielding effects, so that the Fig.9 was the final design.

**Reviewer:** .Fig.9
Fig.9 without the shield does not exactly correspond with the enlarged figure of Fig.1. Does the "collect" in Fig.1 still exist in Fig.9?

**Authors:** Yes. Some electrons may get out of the shield (Fig.9) through the clearance between the sample and shield; but it will be a small fraction. The fraction should be far less than that through the aperture to be CMA.
Anew design is redrawn. The shield and cone of the electron gun are consisting of the collector: They are floating from the ground and connected to the electrometer to measure the all current flowing into these electrodes. But you don't appreciate our design, so that goto added a ring for the more efficient collector to gain a few percent or less efficiencies.